Supporting Information

Electrochemical and kinetic studies on the electrolytic extraction of Gd on Bi electrode in LiCl-KCl melt

Li Ding [a,b,1], Xin Kong [a,1], Yan Gong [a], Shanxin Yang [b], Yongde Yan [a,b,*], Yuan Deng [c,d,*], Yun Xue [b], Kai Zhu [a,*], Fuqiu Ma [b], Wei Liu [c]

[a] Key Laboratory of Superlight Materials and Surface Technology, Ministry of Education, College of Materials Science and Chemical Engineering, Harbin Engineering University, Harbin 150001, Heilongjiang, China

[b] Yantai Research Institute & Graduate School, Harbin Engineering University, Yantai 264006, Shandong, China

[c] Fudan University, Shanghai, 200433, China

[d] Inner Mongolia Rare Earth Functional Materials Innovation Center, Baotou 014010, Inner Mongolia, China

[*] Corresponding author

E-mail address: y5d2006@hrbeu.edu.cn

Extraction and recovery of rare earth elements by molten salt electrolysis

Abstract: As rare earths and their products emerge in various fields due to their excellent properties, the global demand for rare earths is increasing day by day. The existing capacity cannot meet the supply balance. Whether improving production technology or recovering secondary resources, comprehensive and in-depth researches on rare earths are necessary. This paper reviews the electroextraction of rare earths on various electrodes in recent years, focusing on the electrochemical, thermodynamic, and reaction kinetics between rare earth ions and electrodes.

1. Introduction

Rare earths are known to be critical materials of strategic importance, and due to their unique properties, applications can be seen in everything from large spacecraft to small smart products such as the Apple Watch. With the rapid development of the economy, society's demand for new technological products is driving the dramatic expansion of the rare earth market.[1, 2] As a result, the balance of supply based on current extraction and utilization methods is about to be upset. To solve this problem, efficient mining and extraction technologies, as well as recycling strategies conducive to the sustainable development of rare earths, are urgently needed. However, rare earth elements (REEs) have great chemical activity and a strong affinity for oxygen, making extraction or recovery of REEs under normal conditions a very big challenge.

Due to the chemical properties of REEs, they cannot be stable in aqueous system. Therefore, the extraction and recovery of REEs need to be based on non-aqueous media. Electrochemical method using high-temperature molten salt as a medium to prepare active metals can provide an opportunity for the extraction and recovery of REEs.[3-5] As shown in Fig. S1, molten salt electrolysis, which achieves ion reduction and phase separation through electrochemical reactions in an electrolytic cell, is an ideal choice for rare earth preparation and recovery. The

simple process has attracted widespread attention to the molten salt electrolysis of rare earth. There are many factors that affect molten salt electrolysis, such as temperature, current, voltage, etc., but the essence is to control the electrolysis process through two physical media: electrodes and molten salt electrolyte. This phenomenon has led to a divergence of research directions, with one focusing on electrolytes and the other exploring around electrodes.[6-13] Compared to the former, the electrochemical exploration of rare earth electrolysis in molten salt on various electrodes has aroused considerable interest among researchers and great progress has been made in this area.

This paper summarizes the findings from diverse studies using distinct electrodes and various rare earth ions, with a focus on the electrochemical behavior, thermodynamic and kinetic properties of rare earth ions on the electrodes. In order to better understand the research of rare earths on electrodes, the findings could be divided into the reaction on solid electrodes and the extraction on liquid electrodes based on the research focus. Furthermore, the data obtained from these studies were pooled and analyzed.

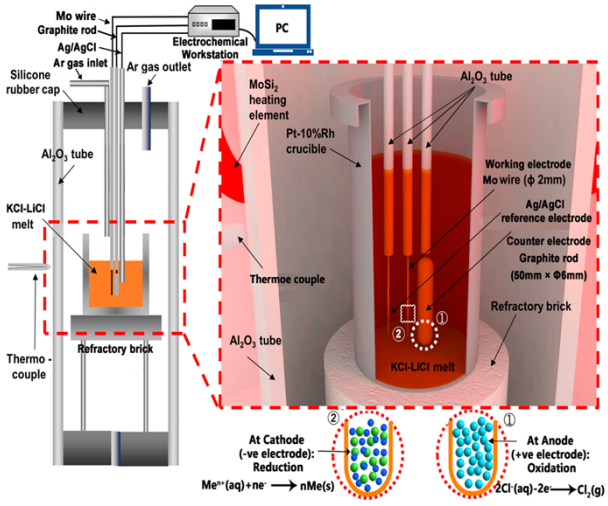

Fig. S1 Schematic diagram of molten salt electrolysis cell.

2. Electrochemical reduction and alloying on solid electrodes

Rare earth is a collective name for 17 elements including scandium (Sc), yttrium (Y) and

lanthanides (Lns). In 1857, Hillebrand et al. successfully prepared rare earth metals by chloride molten salt electrolysis, which opened the prelude to the study of rare earth molten salt electrochemistry[14]. The electrochemical study of molten salt electrolysis of rare earths was initially conducted on inert electrodes such as W and Mo.[15-17] The research on inert electrodes have focused on electrochemical behavior or reduction reactions, ion diffusion, and nucleation. Of course, there are also thermochemical properties and exchange current density measurements, etc., which will be further discussed in the following sections.

2.1 Electrochemistry on inert electrodes

2.1.1 Electrochemical reduction

Yttrium (Y), as the earliest discovered REE, was widely studied in the early days. Hikino et al. studied the electrochemical behavior of Y ions in LiCl-KCl-NaCl eutectic melt and revealed the reaction process of one-step three-electron reduction of Y by calculating the number of transferred electrons.[18] The results of Liu et al. and Han et al. verified this finding and further established the reversibility of the reduction of Y ion.[19, 20] Lanthanum (La) as a typical representative of Ln rare earths had also attracted the attention of researchers. Masset et al. and Fabian et al. investigated the electrochemical reduction of $LaCl_3$ in LiCl-KCl eutectic molten salt by cyclic voltammetry.[21, 22] The results obtained from them indicated that the reduction of La(III) to La is a reversible process at scan rate lower than 1.0 V s^{-1}. Castrillejo et al. and Chandra et al. studied the electrochemical behavior of $CeCl_3$ in the eutectic LiCl-KCL, CaCl-NaCl and LiF-CaF_2 melts, which also supported this discovery of reversible reduction of rare earth ions.[16, 23, 24] Similar studies had also been conducted on elements such as Pr, Dy, Tb.[25-29] As a matter of fact, in molten salts, similar electrochemical properties cause most rare earth ions to react similarly on inert electrodes. Rare earth ions can be classified into two groups based on their reaction characteristics on inert electrodes. One group is represented by La. This

group of REE ions, like La(III) ion, is reduced on an inert electrode by a one-step three-electron reaction and shows similar reaction peaks and approximate reduction potentials in the CV curve (as shown in Fig. S2a). These elements can be referred to as “non-variable” REEs, including gadolinium(Gd),[30] holmium (Ho),[31] erbium (Er),[32] lutetium (Lu),[33] scandium (Sc),[34] and the above references to Ce, Pr, Tb, Dy. Another class is the “variable” REEs composed of Nd, Yb, Sm, Eu, and Tm. Fukasawa et al. and Cordoba et al. found that the electrochemical reduction process of Nd(III) ions to Nd metal consists of two steps: $Nd(III) + e^- \rightarrow Nd(II)$, $Nd(II) + 2e^- \rightarrow Nd$.[35, 36] Later, Xue et al., Kuznetsov et al., and Novodelova et al., in their studies, also found differences in the reduction between Sm, Eu, Tm ions and other rare earth ions, respectively.[37-39] Even though Nd(III), Yb(III), Sm(III), Eu(III), and Tm(III) are all reduced by two steps on the inert electrode, there are differences among them. As shown in Fig. S2b and c, the deposition reaction of Nd can be clearly observed from the CV curves obtained in LiCl-KCl molten salt, whereas only the redox peaks attributed to Sm(III)/Sm(II) can be detected and observed due to the fact that the deposition potentials of Sm are more negative than those of Li. This means that Sm, Eu and Tm metals cannot be prepared by conventional molten salt electrolysis.

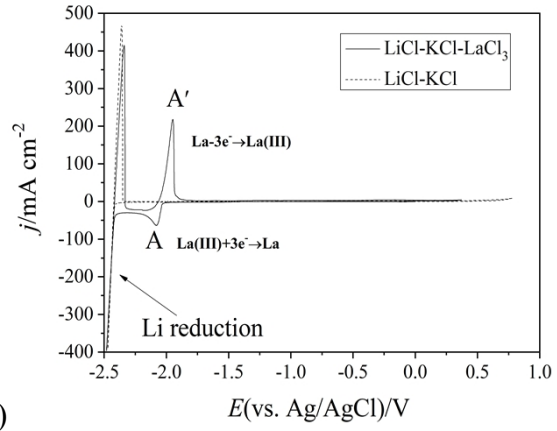

(a)

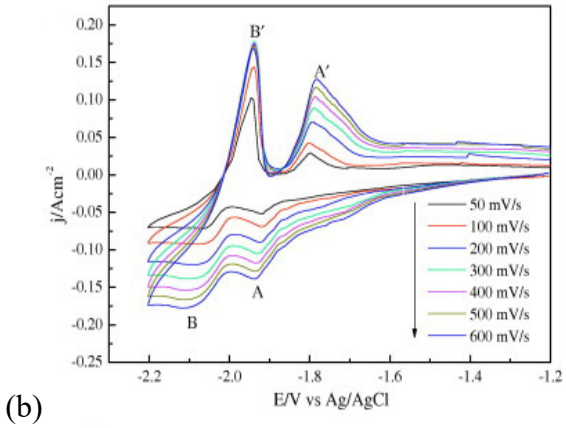

(b)

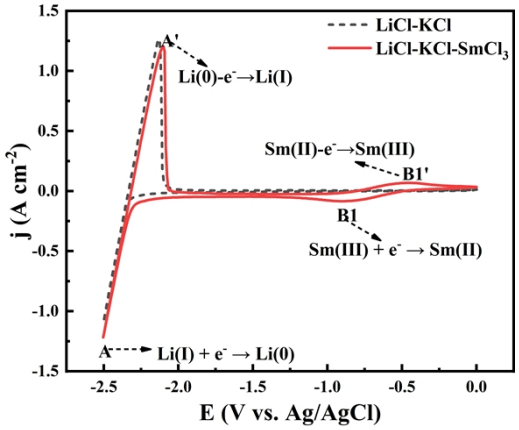

(c)

Fig. S2 CV curves of rare earth ions on W electrode in LiCl-KCl melts: (a) La; (b) Nd; (c) Sm.

2.1.2 Diffusion coefficient

REEs do not stabilize as ions in the molten salt but form complexes with F^- or Cl^- ions in the molten salt.[40, 41] This causes the movement of rare earth ions in molten salt to be different from that in solution. The diffusion of rare earth ions in molten salt affects the electrode reaction, and its diffusion coefficient is the basis of optimizing molten salt electrolysis and developing spent fuel reprocessing. Therefore, the diffusion of rare earth ions has become the focus of researchers. As displayed in Fig. S3, in a typical case, Su and his partner measured the diffusion coefficient of Dy(III) ions by CVs based on the Berzin-Delahay equation, and the its value at 773k was 5.10×10^{-6} cm^2 s^1.[42] Smolenski et al. determined the diffusion coefficient of Yb(III) ions in LiCl-KCl, NaCl-KCl, and CsCl molten salts by the CV method in a Yb(III)/Yb(II) soluble-soluble reaction. They found that the diffusion coefficient of ytterbium

(III) ions becomes smaller as the radius of the alkali metal cation increases from Li to Cs, which can be expressed as $\log D_{Yb(III)} = -6.07 - \frac{0.17}{r} \pm 0.02$.[43] Castrillejo et al. measured the diffusion coefficient of Ho(III) ion in the temperature range of 763 to 963 K by chronopotentiometry and Sand's equation, and further revealed the relationship between the diffusion coefficient and temperature. It can be expressed as $\log D_{Ho(III)} = -2.89(\pm 0.033) - 1646(\pm 24.6)T^{-1}$.[31] There are many other electrochemical methods for measuring ion diffusion coefficients such as LSV and NPV,[44, 45] however, the essence is to induce fluctuations in current density *j* and/or electrode potential φ via an electric perturbation.[46] In other words, the researchers either imposed a potential program and observed the temporal variation of the current, or conversely imposed a current program and monitored the evolution of the electrode potential. Besides, the diffusion coefficients can also be evaluated from electrochemical impedance spectroscopy, where the straight line at low frequency of a typical Nyquist plot is attributed to the ionic diffusion.[34, 47-52]

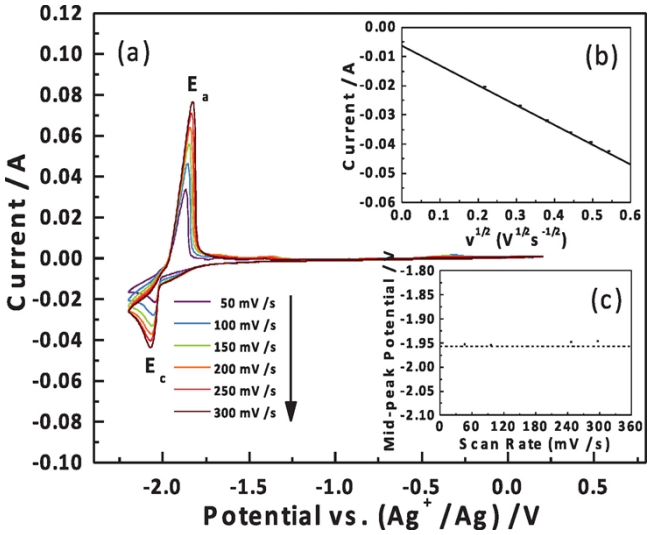

Fig. S3 (a) CVs for 3.73×10^{-5} mol cm^{-3} $DyCl_3$ in LiCl-KCl melts at various scan rates. (b) Plot of the cathodic peak current as a function of the square root of the scan rate. (c) Mid-peak potential as a function of the scan rate.[42] (Reproduced with permission from the author.)

2.1.3 Nucleation

Nucleation studies are fundamental to understanding the growth of rare earths deposited in melts, yet the high temperature environment is a major challenge. The chronoamperometry technique capable of responding to nucleation feedbacks offer opportunities for nucleation studies and have attracted the attention of researchers.[31, 53] Tang and Pesic investigated the nucleation mechanism of La deposition on a Mo substrate according to the Scharifker-Hill non-dimensional model. The instantaneous nucleation and dendritic growth mechanism of La were revealed through comparative analysis of experimental data and theoretical models.[17] Subsequently, Tang and his partner again studied the nucleation process of Nd. As shown in Fig. S4, they revealed the unique nucleation mechanism of Nd by a combination of electrochemical methods and SEM characterization. It was found that the nucleation and growth of Nd was progressive at low initial $NdCl_3$ concentrations, whereas at higher concentrations the related mechanism is instantaneous.[54] Zhang et al. revealed the instantaneous nucleation mechanism of Yb by means of the current-time dimensionless curves derived from chronoamperometry curve, and further explained the three stages of electrochemical nucleation. The three stages are the charging process of electrode double layer, the nucleation process of electrocrystallization and the electrodeposition process controlled by diffusion.[55]

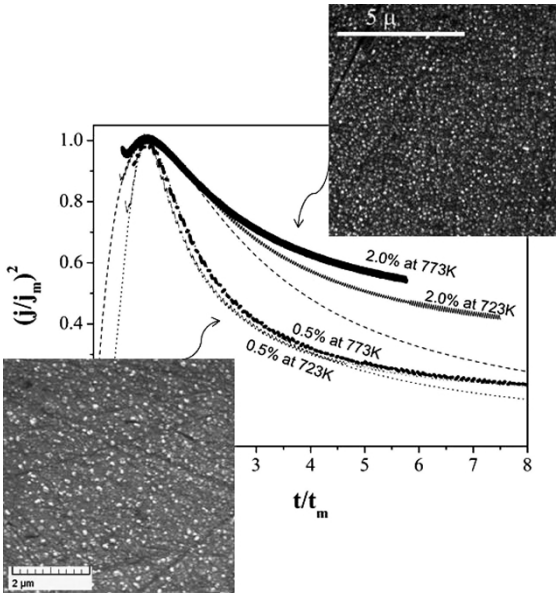

Fig. S4 Comparison of the dimensionless experimental data for several overpotentials, derived from the current-time transients, with the theoretical models for instantaneous (dashed line) and progressive (dotted line) nucleation mechanisms.[54] (Reproduced with permission from the author.)

In order to better understand the electrochemical studies of rare earths on inert electrodes, we summarized these findings and presented them in Table S1. It can be seen that the diffusion coefficients of rare earth ions in molten salts are basically of an order of magnitude at the same temperature. Due to the similar electrochemical properties, the reduction peak potentials of the non-variable rare earth ions are similar.

Table S1 Reduction processes, diffusion coefficients, and nucleation of rare earth ions on inert electrodes.

Rare earth ions	Ions reduction	Diffusion coefficient / 10^5 cm^2 s^{-1}	Reduction peak potential / V	Type of nucleation
La[17]	One-step reduction	1.70 (773 K)	-2.08 (vs. Ag/AgCl)	Instantaneous nucleation
La[56]		-	-2.05 (vs. Ag/AgCl)	-
La[57]		2.1±0.5 (773 K)	-1.0 (vs. Pt Q. R. E)	-
Ce[51]	One-step reduction	2.383 (954 K)	-1.95 (vs. Ag/AgCl)	-
Ce[58]		1.398 (773 K)	-2.1 (vs. Pt Q. R. E)	-
Ce[52]		3.48±0.02 (963 K)	-2.0 (vs. Ag/AgCl)	-
Pr[26]	One-step reduction	1.375 (748 K)	-3.2 (vs. Cl_2/Cl^-)	-
Pr[25]		-	-1.6 (vs. Pt Q. R. E)	-
Nd[54]	Two-step	-	-1.87/-2.03 (vs.	Instantaneous

	reduction		Ag/AgCl)	nucleation / Continuous nucleation
Nd[59]		2.35 (773 K)	-1.858/-1.978 (vs. Ag/AgCl)	-
Nd[60]	One-step reduction	0.399 (823 K)	-1.45 (vs. Pt Q. R. E)	-
Sm[37]	Two-step	2.33 (803 K)	-0.91 (vs. Ag/AgCl)	-
Sm[24]	reduction	-	-1.25 (vs. Pt Q. R. E)	-
Eu[61]	Two-step reduction	-	0.197 (vs. Ag/AgCl)	-
Gd[30]	One-step	0.88 (723 K)	-2.23 (vs. Ag/AgCl)	-
Gd[62]	reduction	-	-2.05 (vs. Ag/AgCl)	-
Tb[28]	One-step reduction	0.756 (748 K)	-2.12 (vs. Ag/AgCl)	Instantaneous nucleation
Tb[63]		2.06±0.4 (887 K)	-	-
Dy[64]	One-step reduction	11.22 (1243 K)	-0.13 (vs. Pt Q. R. E)	Instantaneous nucleation / Continuous nucleation
Dy[65]		11.59 (1103 K)	-0.75 (vs. Pt Q. R. E)	Instantaneous nucleation
Dy[27]		6.95±0.04 (1203 K)	-1.75 (vs. Pt Q. R. E)	-
Ho[66]	One-step reduction	-	-2.03 (vs. Ag/AgCl)	-
Er[32]	One-step	1.48 (823 K)	-	Instantaneous nucleation
Er[67]	reduction	2.01 (873 K)	-	-
Tm[68]	Two-step reduction	50 (Tm(III) 673 K) 46 (Tm(II) 673 K)	-	Instantaneous nucleation / Continuous nucleation
Yb[43]	Two-step	1.0±0.1 (723 K)	-1.762 (vs. Cl_2/Cl^-)	-
Yb[69]	reduction	2.57±0.02 (1113 K)	-	-
Lu[70]	One-step reduction	-	-1.89 (vs. Ag/AgCl)	-
Sc[34]	One-step reduction	-	-2.05 (vs. $Pt/PtO_x/O^{2-}$)	-
Y[18]	One-step	0.33 (723 K)	0.35 (vs. Li/Li^+)	-
Y[19]	reduction	0.565 (723 K)	-2.08 (vs. Ag/AgCl)	Instantaneous nucleation

2.2 Alloying on active electrodes

The extraction of rare earths on active electrodes is essentially the preparation of rare earth alloys. Rare earths often exhibit their excellent properties or play a crucial role in industry in the form of alloy compounds. Preparation of rare earth alloys by electrolysis on active electrodes avoids the burning loss of rare-earth metals in the case of alloys prepared by smelting. Rare-earth molten salt electrolysis on active electrodes has therefore received much attention, and the electrochemical alloying of rare earth ions on active electrodes has been further investigated. According to the characteristics of the active electrode, the molten salt electrolytic preparation or electrochemical alloying research studies can be divided into those on liquid active electrodes and those on solid active electrodes. The former we will introduce in detail in later chapters, and the latter is what we focus on in this chapter. Induced by the demand for rare earth alloys, research on alloying on solid state active electrodes has focused on Mg, Ni, and Al electrodes.

a) Mg electrode

Yang et al. investigated the selective extraction and alloying process on Mg electrodes in LiCl-KCl-$GdCl_3$-$DyCl_3$ melts at 773 K. In this case, only the formation of Mg_3Dy was observed. The result of ICP-AES indicated that the extraction efficiency of Dy reached 98.4%. In addition, the growth rate of Mg_3Dy was measured.[71] In order to understand the electrochemical process of RE-Mg alloys formation in molten salts, Tang et al. studied the electrochemical behavior of Mg(II) and Pr(III) ions by co-deposition method. It was found that only one Pr-Mg intermetallic compound was formed during co-deposition, and $Mg_{12}Pr$ alloy was prepared by potentiostatic electrolysis at −1.85 V.[72] Ji et al. investigated the electrochemical alloying of La(III) ions by Mg film electrodes, and found the underpotential deposition of La(III) and the formation of three Mg-La intermetallic compounds. Moreover, they achieved phase control of Mg-La alloy by changing the electrolysis potential.[73]

Interestingly, Yang and his partners discovered the chlorination of $MgCl_2$ while studying the preparation of rare earth alloys using Gd_2O_3, and revealed the component changes during chlorination and alloying by XRD analysis.[74]

b) Ni electrode

Xie et al. studied the deposition process of Y on Ni. The generation of Y-Ni alloy was verified by CV tests at different temperatures and the effects of current density and temperature on the electrolytic preparation were further explored.[75] Nohira et al. investigated the electrochemical formation and phase control of Pr-Ni Alloys in a molten LiCl-KCl-$PrCl_3$ system. It was found that PrNi intermetallic compounds were first formed on thin Ni electrodes followed by phase transition during continuous deposition of Pr. Furthermore, the rapid formation of $PrNi_2$ induced by Pr diffusion was determined by through morphological and crystallographic investigations using transmission electron microscopy and electron diffraction.[76] Yasuda et al. studied the electrochemical formation of Dy-Ni alloys in molten NaCl-KCl-$DyCl_3$. They found that only one pair of redox peaks attributed to the Dy-Ni alloy could be observed on the CV curves due to the superposition of reaction currents on the Ni electrode. Subsequently, the formation of four Dy-Ni alloy phases was determined by OCP.[77] Hua and his colleagues investigated the formation of Nd-Ni alloys in $CaCl_2$-NdCl melts. It was found that unlike that on inert electrodes, Nd undergoes a one-step reduction on Ni electrode and forms three kinds of Ni-Nd alloys.[78]

c) Al electrode

Due to the excellent strength-to-weight ratio and corrosion resistance, RE-Al alloy is widely used in various industries, and its related research has also been favored by researchers. Shi et al. explored electrochemical formation of RE-Al (RE=La, Ce, Gd, Tb, Dy, Ho, Er) alloys in molten salts.[42, 79-83] They determined the stable phase of RE-Al alloys in molten salt by co-

deposition of RE(III) and Al(III) ions, and prepared a variety of RE-Al alloys by potentiostatic and galvanostatic electrolysis. In addition, they developed the rare earth alloys preparation using rare earth oxides as raw materials with the assistance of $AlCl_3$.[79, 81, 82] Castrillejo et al. investigated the preparation of RE alloys (RE=Eu, Dy, Ho, Er, Tm, Lu, Sc) directly on Al electrodes.[31-33, 68, 84-86] They investigated the effects of factors such as potential, temperature, and current density on electrochemical alloying, and prepared various alloys such as $EuAl_4$, $TmAl_3$, and $LuAl_2$ by controlling these factors.

There were many more research efforts that were not listed. In order to better understand the findings on alloying on active electrodes or on the preparation of rare earth alloys, we summarized and displayed them in Table S2. Rare earth alloy phases are diverse, and the preparation of rare earth alloys of a specific composition by controlling the electrolysis conditions on the active electrode or by co-deposition in the molten salt is the most efficient and convenient method.

Table S2 Phase control of rare earth alloys prepared by alloying on active electrodes or co-deposition in molten salts.

Rare earth ion	Electrode	Temperature / K	Applied current / potential	Alloy phase
Pr[87]	Mg	823	-100 mA	$PrMg_3$
Dy[71]	Mg	773	-1.9 V (vs. Ag/AgCl)	$DyMg_3$
Tm[88]	Mg	833	-594 mA cm^{-2}	$TmMg_2$, Tm_5Mg_{24}
Lu[70]	Mg	873	-2.2 V (vs. Ag/AgCl)	LuMg, Lu_5Mg_{24}
Yb[89]	Mg	773	-1.85 V (vs. Ag/AgCl)	$YbMg_2$
La[90]	Ni	1123	-10 A cm^{-2}	LaNi
Nd[91]	Ni	973	0.25 V (vs. Na^+/Na)	$NdNi_2$
Nd[92]	Ni	1113	-35 mA cm^{-2}	$NdNi_2$, $NdNi_3$
Pr[93]	Ni	723	0.5 V (vs. Li^+/Li)	$PrNi_2$
Pr[94]	Ni	1123	0.2 V (vs. Li^+/Li)	$PrNi_2$
Pr[95]	Ni	873	-2 V (vs. Ag/AgCl)	$PrNi_5$, Pr_2Ni_7, $PrNi_3$, $PrNi_2$
Sm[96]	Ni	723	0.1 V (vs. Li^+/Li)	$SmNi_2$

Sm[37]	Ni	1120	-200 mA cm^{-2}	$SmNi_3$
Dy[77]	Ni	973	0.25 V (vs. Na^+/Na)	$DyNi_2$
Dy[97]	Ni	700	0.55 V (vs. Li^+/Li)	$DyNi_2$
Dy[98]	Ni	1123	0.2 V (vs. Li^+/Li)	$DyNi_2$, $DyNi_3$
Tb[99]	Ni	723	0.7 V (vs. Li^+/Li)	$TbNi_2$
Gd[92]	Ni	1113	-32 mA cm^{-2}	$GdNi_2$, GdNi
Ho[100]	Ni	1023	-2.2 V (vs. Ag/AgCl)	Ho_2Ni_{17}, $HoNi_5$, $HoNi_2$
Yb[93]	Ni	723	0.1 V (vs. Li+/Li)	$YbNi_2$
Y[101]	Ni	723	0.31 V (vs. Li+/Li)	Y_3Ni_2, YNi
Y[102]	Ni	873	-150 mA cm^{-2}	YNi_2, YNi
La[103]	Al	798	-1.5 V (vs. Ag/AgCl)	La_3Al_{11}
Sc[86]	Al	723	-0.175 A	Sc_2Al
Lu[33]	Al	723	-2.35 V (vs. Ag/AgCl)	$LuAl_2$, $LuAl_3$
Sm[104]	Al	773	-2.1 V (vs. Ag/AgCl)	$SmAl_2$
Eu[85]	Al	723	-2.45 V (vs. Ag/AgCl)	$EuAl_4$
Dy[84]	Al	723	-2.98 V (vs. Cl_2/Cl^-)	$DyAl_3$
Tb[82]	Al	903	-1.6 V (vs. Ag/AgCl)	$TbAl_3$
Ho[105]	Al	773	-2.2 V (vs. Ag/AgCl)	$HoAl_{17}$
Er[32]	Al	723	-3.08 V (vs. Cl_2/Cl^-)	$ErAl_3$
Tm[106]	Al	823	-2.7 V (vs. Cl_2/Cl^-)	$TmAl_2$, $TmAl_3$
La[107]	W	1023	-1.26 A cm^{-2}	$LaMg_{12}$, La_2Mg_{17}
La[108]	Mo	943	-12.7 A cm^{-2}	La_2Mg_{17}, $LaMg_3$
Pr[72]	W	913	-6 A cm^{-2}	$PrMg_3$, $PrMg_{12}$
Dy[109]	Mo	873	-2.2 V (vs. Ag/AgCl)	$DyMg_3$
Yb[110]	Mo	933	-4 A	$YbMg_2$
La[111]	Mo	1123	-3.2 V (vs. Ag/AgCl)	$LaNi_5$
Ce[24]	W	1113	-1.79 V (vs. Pt)	Ce_3Al, CeAl
Ce[79]	Mo	773	-1.9 V (vs. Ag/AgCl)	Ce_3Al_{11}
Er[112]	Mo	773	-320 mA cm^{-2}	Al_2Er, Al_2Er_3, Al_4Li_9
Nd[113]	W	1133	-1.88 V (vs. Pt)	Nd_3Al
Sm[114]	W	1223	-0.7314 A cm^{-2}	$SmAl_2$, $SmAl_3$
Eu[115]	W	1113	-1.1 V (vs. Pt)	$EuAl_4$
Nd[116]	W	773	-1.718 V (vs. Ag/AgCl)	Nd_5Bi_3
Y[117]	Mo	1323	-8 A cm^{-2}	Y_2Al
Pr[118]	Mo	923	-5 A	Co_2Pr

3. Electrolytic extraction on liquid electrodes

Compared with solid electrodes, liquid electrodes have a number of fascinating properties such as a more positive deposition potential, good depolarization effect and the ability to prepare homogeneous alloy products.[4, 5] Due to the advantages of liquid electrodes, the electrolytic extraction of rare earths or the preparation of their alloys using liquid metals as cathodes has been the focus of attention. Of course, to be clear, researchers are paying attention to the electrolytic extraction on liquid electrodes not only because it provides a more efficient method for extracting rare earth alloys, but also because it is the key to promoting the development of advanced nuclear fuel cycles.[119, 120] Many efforts have been made to reveal the electrolytic reduction and extraction processes on liquid electrodes, and we will present the findings of these works in terms of kinetic and thermodynamic studies.

3.1 Reduction potential

The difference in reduction potential on the liquid electrode determines the deposition sequence of rare earth ions on different cathodes. As shown in Fig. S5, Yang et al. determined the reaction priority of Nd ions on Al, Cd, Pb, Zn, Ga, Sn, and Bi electrodes by measuring the reduction potential on the CV curves. It was found that Zn, Ga, Sn and Bi electrodes have a strong depolarization effect on Nd and the order of depolarization effect is Bi>Sn>Ga>Zn>Pb>Al>Cd.[121] In a study of electrolytic extraction of Ce and Nd on liquid Ga electrodes, Liu et al. found that the reduction potentials of Ce(III) and Nd(III) ions differed by only 0.063 V. Subsequently, the relationship between the apparent standard potentials ($E^{*}_{Ce(III)/Ce}$ and $E^{*}_{Nd(III)/Nd}$) as a function of temperature was revealed by means of the semi-deriviative as well as the Nernst equation.[122] Luo et al. studied the kinetics process of Tb(III)/Tb couple at liquid Zn electrode, and found that the reduction potential of Tb(III) ions in liquid Zn is move positive than that in W electrode due to the diffusion of Tb into the electrode and the low activity in the metal phase.[123] In fact, from the point of view of underpotential deposition,

the formation of a monolayer deposition layer in the underpotential region is caused by the fact that the interaction between the deposited rare earth atoms and the base cathode atoms is greater than that between the deposited rare earth atoms. The formation of this submonolayer deposition layer and the continued diffusion of rare earth atoms macroscopically manifests itself in the fact that the reduction potential of rare earths at the liquid electrode is more positive than that at the inert electrode.[5, 124, 125]

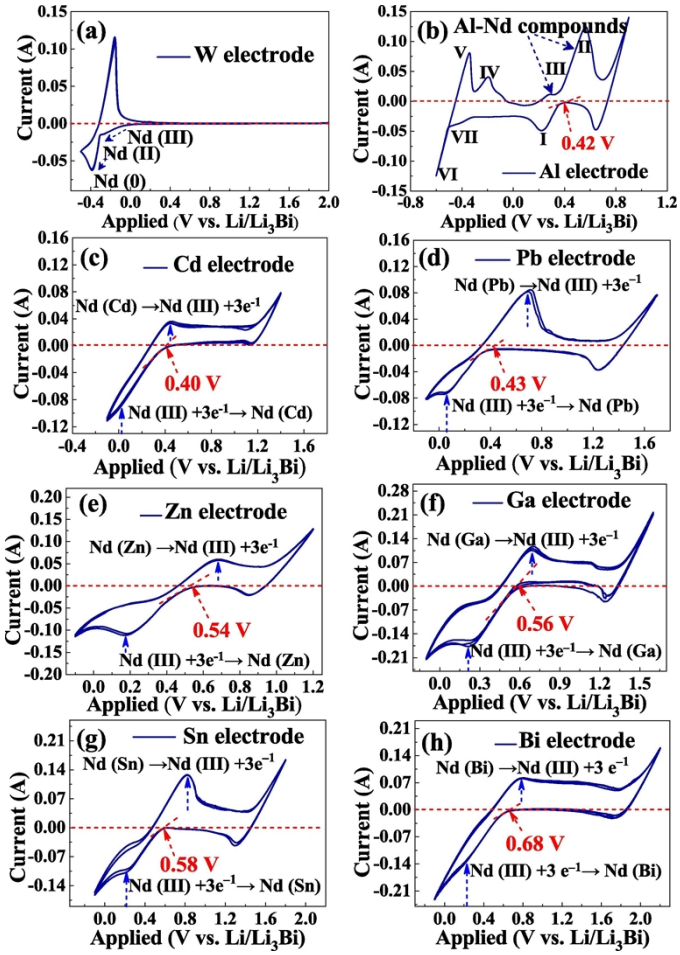

Fig. S5 Cyclic voltammograms of Nd^{3+} on various electrodes (W, Al, Cd, Pb, Zn, Ga, Sn, and Bi) in the LiCl-KCl-$NdCl_3$ (1.0 wt%) melts at 723 K.[121] (Reproduced with permission from the author.)

3.2 Exchange current density

The exchange current density is an important parameter reflecting the electrochemical kinetic behavior on the electrode and has therefore received much attention in the study of

liquid electrodes. As shown in Fig. S6, in a typical case, Yin et al. measured the exchange current density of Ln (Ln=La, Ce, Pr, Nd) on liquid Bi electrodes by electrochemical impedance spectroscopy, and found that Ce has a faster reaction rate on Bi electrode at 723 K. Furthermore, they verified the measurement results by galvanostatic pulse, and further revealed the temperature dependence of the exchange current density and the ionic reaction rate sequence: Ce>Nd>La>Pr.[126] Yang et al. studied the electrochemical kinetics of Nd(III) ions on various liquid electrodes by Tafel and linear polarization methods. It was found that Nd ions have the fastest reaction rate at the Cd electrode and the kinetic ordering of the electrodes is Pb<Sn<Bi<Ga<Al<Zn< Cd.[121] Interestingly, Kwon et al. developed atomistic-level kinetics model using first-principles calculations, and found identified a universal relation between exchange current densities and adsorption energy. They achieved the prediction of the exchange current density by thermodynamic adsorption energy solvated rare earth ions in LiCl-KCl eutectic molten salt.[127]

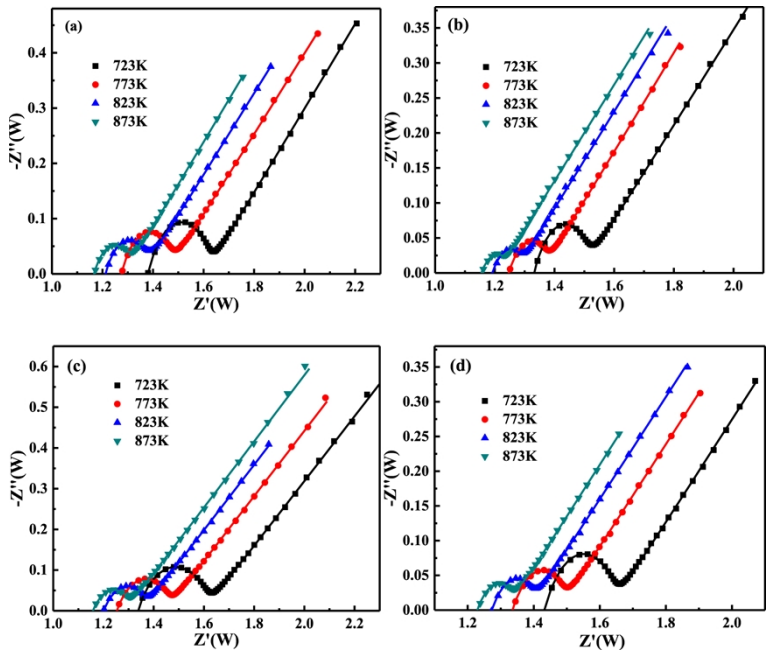

Fig. S6 Measured (dotted line) and fitted (solid line) Nyquist plots for (a) $LaCl_3$ (1.2×10^{-4} mol cm^{-2}), (b) $CeCl_3$ (1.42×10^{-4} mol cm^{-2}), (c) $PrCl_3$ (1.39×10^{-4} mol cm^{-2}) and (d) $NdCl_3$ (1.88×10^{-4} mol cm^{-2}) in LiCl-KCl melt on liquid Bi electrodes at temperatures of 723, 773, 823 and 873 K, respectively.[126] (Reproduced with permission from the author.)

3.3 Activity and activity coefficient

The activity and activity coefficient can reflect the real concentration change in the melt. The determination of the activity and activity coefficient of rare earths in liquid electrodes is based on the needs of the industrial construction of rare earth preparation and spent fuel electrolysis. Changes in the components of an alloy cause a change in its potential. Kim et al. constructed an electrochemical cell by two half-reactions. The electrochemical cell was shown below:

$$Ln\,|\,LiCl-KCl-LnCl_3\,|\,Ln(Me)$$

And the logarithm of the activity coefficient was related to the emf between pure metal and alloyed metal through the following expression:

$$\log\gamma_{Ln(Me)}=\frac{n\cdot F\cdot emf}{2.3RT}-\log X_{Ln(Me)}$$

They evaluated the activity coefficients of Nd in Al by the cyclic voltammetry technique, the coulometric additions method and the direct use of an Al-Nd alloy. It was found that the results determined by the three methods were in good agreement, and the variation of the activity coefficient of Nd in Al(l) as a function of the temperature could be expressed as $\log\gamma_{Nd(Al)}=9.81-17134/T$.[36] Coulometric addition (or called coulomb titration) makes it feasible to continuously measure the activity and activity coefficient for different Ln concentrations, and is considered to be more accurate compared to other methods from the perspective of in-situ measurement.[12, 128, 129] Therefore, this method was frequently used in the determination of activity coefficients in melts. Liu et al., Yin et al, Wang et al, and Smolenski et al. determined the activity coefficients of Ln (Ln=La, Ce, Pr, Nd, Sm) in liquid Ga, Bi, Al, Zn, Sn, Ga-Al, and Ga-In by coulomb titration.[5, 11, 62, 122, 126, 130-133]

3.4 Solubility

Coulomb titration also provides an opportunity to determine the solubility of rare earth elements, especially lanthanides, in liquid electrodes. In a typical case, Liu et al. first measured the formation potential of the alloy by galvanostatic electrolysis and then, as shown in Fig. S7, obtained the maximum molar fractions of Ce and Nd on the liquid Ga electrodes by the accumulation of multiple Coulomb titrations.[122] This mole fraction can be considered as the solubility of Ga for Ce and Nd. Li et al. also determined the solubility of Dy on Sn by this method, and the value was 3.95×10^{-2}.[134] Xu et al. revealed the dependence of the activity coefficient on temperature by coulomb titration, and further obtained the dependence of solubility on temperature by the relationship between activity and mole fraction.[135]

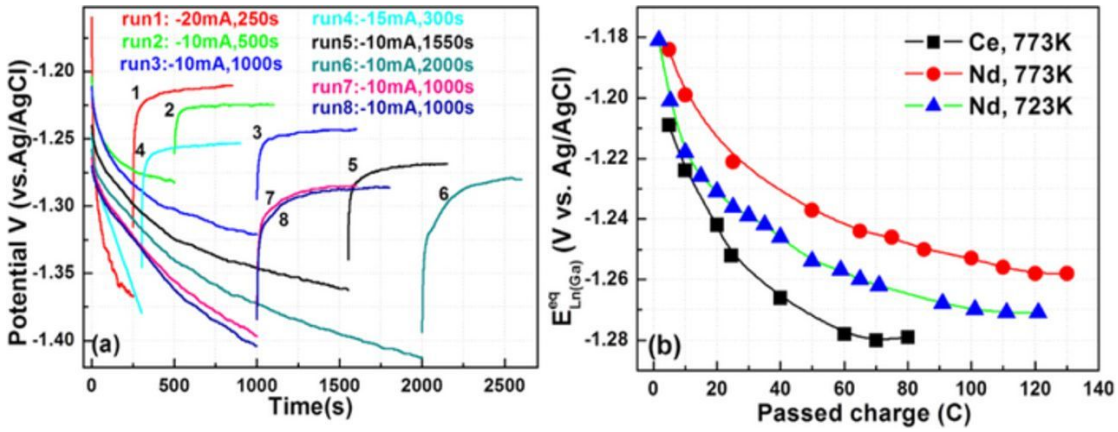

Fig. S7 (a) Galvanostatic electrolysis at different runs and corresponding OCP curves for Ce metal on the liquid Ga electrode. (b) The equilibrium potentials of Ln(Ga) electrode after each run of electrolysis.[122] (Reproduced with permission from the author.)

The kinetic and thermodynamic parameters of rare earth ions on these liquid electrodes were summarized and shown in Table S3. It can be seen that the kinetic and thermodynamic work on the liquid electrode is still insufficient, and the data of Ho, Er, Tm and other rare earth elements on the liquid electrode are missing. There are orders of magnitude differences in the data even on the same liquid electrode due to differences in test methods and experimental conditions. The kinetic and thermodynamic studies of rare earth ions on liquid electrodes need to be optimized.

Table S3 Kinetic and thermodynamic parameters of rare earth ions on liquid electrodes.

Rare earth ions	Liquid electrode	Temperature / K	Activity coefficient	Exchange current density	Solubility
La[136]	Pb/Pb-Ga	823	3.75×10^{-12} /1.51×10^{-13}	0.0057/0.0062 A cm^{-2}	-
La[126]	Bi	723	1.02×10^{-17}	68.99 mA cm^{-2}	-
Ce[122]	Ga	773	2.43×10^{-15}	-	0.00845
Ce[126]	Bi	723	2.4×10^{-14}	93.12 mA cm^{-2}	-
Ce[10]	Bi/Sn/Zn	773	3.16×10^{-14} /1.82×10^{-12} /9.05×10^{-10}	-	-
Pr[137]	Sn	763	-	0.008 A cm^{-2}	-
Nd[122]	Ga	773	7.08×10^{-15}	-	0.0077
Nd[138]	Ga-Al	773	3.1710^{-12}	-	-
Nd[121]	Ga/Bi/Sn/Zn/Pb /Cd	723	-	0.137/0.146/0.142/0.058/0.154/0.134 A cm^{-2}	-
Gd[139]	Pb	723	-	0.0292 A cm^{-2}	-
Dy[134]	Sn	773	-	-	0.0395

4. Conclusions and prospect

The application of molten salt electrolysis in industrial production is very mature, which benefits from the in-depth study of rare earth ions in molten salt and electrodes. These studies reveal the existence state of rare earth ions in molten salts and the electrolysis reaction process on electrodes, and prompted the establishment of classic methods such as nucleation analysis based on chronopotentiometry, activity measurement based on coulomb titration, and solubility measurement based on pulse electrolysis. These massive basic data from diverse studies have built a firm foundation for the development of molten salt electrochemistry, while also providing reliable support for the recovery of secondary rare earth resources. Although research on the extraction and recovery of rare earth elements through molten salt electrolysis has been continuously advancing, the related work lacks novelty and attractiveness. Current innovative research for molten salt electrolysis can be focused on the design of electrode materials with

selective extractability, coordination chemical analysis of rare earth ions, and exploration of functional electrolytes, and further considers the feasibility of practical application.

Reference

1. C. Ramprasad, W. Gwenzi, N. Chaukura, N. Izyan Wan Azelee, A. Upamali Rajapaksha, M. Naushad and S. Rangabhashiyam, *Chem. Eng. J.*, 2022, **442**, 135992.
2. J. Chen, S. Sun, G. Tu and F. Xiao, *Miner. Eng.*, 2023, **204**.
3. W. Han, M. Li, M.-L. Zhang and Y.-D. Yan, *Rare Met.*, 2016, **35**, 811-825.
4. S.-Q. Jiao, H.-D. Jiao, W.-L. Song, M.-Y. Wang and J.-G. Tu, *Int. J. Miner., Metall. Mater.*, 2020, **27**, 1588-1598.
5. T.-q. Yin, L. Chen, Y. Xue, Y.-h. Zheng, X.-p. Wang, Y.-d. Yan, M.-l. Zhang, G.-l. Wang, F. Gao and M. Qiu, *Int. J. Miner., Metall. Mater.*, 2020, **27**, 1657-1665.
6. Y. K. Zhong, Y. L. Liu, K. Liu, L. Wang, L. Mei, J. K. Gibson, J. Z. Chen, S. L. Jiang, Y. C. Liu, L. Y. Yuan, Z. F. Chai and W. Q. Shi, *Nat Commun*, 2021, **12**, 5777.
7. Y.-L. Liu, J.-H. Lan, L. Wang, S.-L. Jiang, Y.-C. Liu, Y.-K. Zhong, D.-W. Yang, L. Zhang and W.-Q. Shi, *Electrochim. Acta*, 2022, **404**.
8. E. V. Nikolaeva, I. D. Zakiryanova and A. L. Bovet, *J. Electrochem. Soc.*, 2022, **169**.
9. S. Jiang, Y. Liu, L. Wang, Z. Chai and W. Q. Shi, *Chemistry*, 2022, DOI: 10.1002/chem.202201145.
10. J. W. Park, H. L. Cha and J.-I. Yun, *J. Electrochem. Soc.*, 2022, **169**, 043517.
11. K. Liu, Y.-L. Liu, Z.-F. Chai and W.-Q. Shi, *Sep. Purif. Technol.*, 2021, **265**, 118524.
12. S. Im, N. D. Smith, S. C. Baldivieso, J. Gesualdi, Z.-K. Liu and H. Kim, *Electrochim. Acta*, 2022, **425**, 140655.
13. S. Vandarkuzhali, M. Chandra, S. Ghosh, N. Samanta, S. Nedumaran, B. Prabhakara Reddy and K. Nagarajan, *Electrochim. Acta*, 2014, **145**, 86-98.
14. B. Mishra and D. L. Olson, *J. Phys. Chem. Solids*, 2005, **66**, 396-401.
15. Y. Castrillejo, M. R. Bermejo, E. Barrado, A. M. Martınez and P. Dıaz Arocas, *J. Electroanal. Chem.*, 2003, **545**, 141-157.
16. Y. Castrillejo, M. R. Bermejo, R. Pardo and A. M. Martı´nez, *J. Electroanal. Chem.*, 2002, **522**, 124-140.
17. H. Tang and B. Pesic, *Electrochim. Acta*, 2014, **119**, 120-130.
18. S. Hikino, G. Xie, K. Ema and Y. Ito, *J. Electrochem. Soc.*, 1992, **139**, 1820-1824.
19. K. Liu, W. Wang, Y. Ma, M. Kang and B. Wang, *J. Electrochem. Soc.*, 2020, **167**.
20. W. Han, Q. Zhao, J. Wang, M. Li, W. Liu, M. Zhang, X. Yang and Y. Sun, *J. Rare Earths*, 2017, **35**, 90-97.
21. P. Masset, R. J. M. Konings, R. Malmbeck, J. Serp and J.-P. Glatz, *J. Nucl. Mater.*, 2005, **344**, 173-179.
22. C. P. Fabian, V. Luca, P. Chamelot, L. Massot, C. Caravaca and G. R. Lumpkin, *J. Electrochem. Soc.*, 2012, **159**, F63-F67.
23. M. Chandra, S. Vandarkuzhali, S. Ghosh, N. Gogoi, P. Venkatesh, G. Seenivasan, B. P. Reddy and K. Nagarajan, *Electrochim. Acta*, 2011, **58**, 150-156.
24. M. Gibilaro, L. Massot, P. Chamelot and P. Taxil, *Electrochim. Acta*, 2009, **54**, 5300-5306.
25. M. Straka, M. Korenko and L. Szatmáry, *J. Radioanal. Nucl. Chem.*, 2011, **289**, 591-593.
26. Y. Castrillejo, M. R. Bermejo, P. Díaz Arocas, A. M. Martínez and E. Barrado, *J. Electroanal. Chem.*, 2005, **575**, 61-74.
27. A. Saïla, M. Gibilaro, L. Massot, P. Chamelot, P. Taxil and A. M. Affoune, *J. Electroanal. Chem.*, 2010, **642**, 150-156.
28. M. R. Bermejo, J. Gómez, A. M. Martínez, E. Barrado and Y. Castrillejo, *Electrochim. Acta*, 2008, **53**, 5106-5112.
29. M. Li, Q. Gu, W. Han, Y. Yan, M. Zhang, Y. Sun and W. Shi, *Electrochim. Acta*, 2015, **167**, 139-146.
30. C. Caravaca, G. de Córdoba, M. J. Tomás and M. Rosado, *J. Nucl. Mater.*, 2007, **360**, 25-31.
31. Y. Castrillejo, M. R. Bermejo, E. Barrado, J. Medina and A. M. Martínez, *J. Electrochem. Soc.*, 2006, **153**, C713-C721.
32. Y. Castrillejo, M. R. Bermejo, E. Barrado and A. M. Martínez, *Electrochim. Acta*, 2006, **51**, 1941-1951.
33. M. R. Bermejo, E. Barrado, A. M. Martínez and Y. Castrillejo, *J. Electroanal. Chem.*, 2008, **617**, 85-100.
34. C. Wang, J. Chen, B. Li, H. Zhao, B. Jin, K. Liu and Q. Han, *J. Rare Earths*, 2022, **40**, 1641-1650.
35. K. Fukasawa, A. Uehara, T. Nagai, T. Fujii and H. Yamana, *J. Nucl. Mater.*, 2011, **414**, 265-269.
36. G. De Córdoba, A. Laplace, O. Conocar, J. Lacquement and C. Caravaca, *Electrochim. Acta*, 2008, **54**, 280-288.
37. Y. Xue, Q. Wang, Y.-D. Yan, L. Chen, M.-L. Zhang and Z.-J. Zhang, *Energy Procedia*, 2013, **39**, 474-479.
38. S. A. Kuznetsov and M. Gaune-Escard, *J. Electroanal. Chem.*, 2006, **595**, 11-22.

39. A. Novoselova and V. Smolenski, *The Journal of Chemical Thermodynamics*, 2012, **48**, 140-144.
40. G. D. Zissi, A. Chrissanthopoulos and G. N. Papatheodorou, *Vib. Spectrosc*, 2006, **40**, 110-117.
41. H. Matsuura, S. Watanabe, T. Sakamoto, T. Kanuma, K. Naoi, M. Hatcho, N. Kitamura, H. Akatsuka, A. K. Adya, T. Honma, T. Uruga and N. Umesaki, *J. Alloys Compd.*, 2006, **408-412**, 80-83.
42. L.-L. Su, K. Liu, Y.-L. Liu, L. Wang, L.-Y. Yuan, L. Wang, Z.-J. Li, X.-L. Zhao, Z.-F. Chai and W.-Q. Shi, *Electrochim. Acta*, 2014, **147**, 87-95.
43. V. Smolenski, A. Novoselova, A. Osipenko, C. Caravaca and G. de Córdoba, *Electrochim. Acta*, 2008, **54**, 382-387.
44. S. A. Kuznetsov, H. Hayashi, K. Minato and M. Gaune-Escard, *Electrochim. Acta*, 2006, **51**, 2463-2470.
45. Z.-h. Wang, D. Rappleye and M. F. Simpson, *Electrochim. Acta*, 2016, **191**, 29-43.
46. X. Li, Y. Zhang, B. Yue, L. Yan, T. Jiang and S. Peng, *J. Mol. Liq.*, 2020, **297**.
47. E. Barsoukov and J. R. Macdonald, *Impedance spectroscopy: theory, experiment, and applications*, John Wiley & Sons, 2018.
48. O. Shirai, T. Iwai, Y. Suzuki, Y. Sakamura and H. Tanaka, *J. Alloys Compd.*, 1998, **271**, 685-688.
49. P. Van Rysselberghe, *JACS*, 1955, **77**, 2349-2350.
50. A. J. Bard, L. R. Faulkner and H. S. White, *Electrochemical methods: fundamentals and applications*, John Wiley & Sons, 2022.
51. Y.-H. Jia, H. He, R.-H. Lin, H.-B. Tang and Y.-Q. Wang, *J. Radioanal. Nucl. Chem.*, 2014, **303**, 1763–1770.
52. D. K. Sahoo, A. K. Satpati and N. Krishnamurthy, *RSC Advances*, 2015, **5**, 33163-33170.
53. E. Budevski, G. Staikov and W. J. Lorenz, *Electrochim. Acta*, 2000, **45**, 2559-2574.
54. H. Tang and B. Pesic, *J. Nucl. Mater.*, 2015, **458**, 37-44.
55. Y. Zhang, B. Cai, X. Wang, R. Wang and Z. Shi, *J. Electroanal. Chem.*, 2022, **926**.
56. D.-B. Ji, Y.-D. Yan, M.-L. Zhang, X. Li, X.-Y. Jing, W. Han, Y. Xue and Z.-J. Zhang, *J. Radioanal. Nucl. Chem.*, 2015, **304**, 1123-1132.
57. M. Matsumiya and S.-i. Matsumoto, *Zeitschrift für Naturforschung A*, 2004, **59**, 711-714.
58. R. Lin, G. Ye, H. He, H. Tang and Y. Ouyang, *J. Rare Earths*, 2012, **30**, 151-154.
59. S. Kim and S.-h. Lee, *Applied Sciences*, 2020, **10**.
60. F. Jiang, N. Ji, W. Huang and H. Fu, *J. Electrochem. Soc.*, 2022, **169**.
61. J. Ge, Q. Yang, Y. Wang, W. Zhuo, M. Du and J. Zhang, *J. Electrochem. Soc.*, 2020, **167**.
62. Y. Wang, M. Quan, S. Zhang, Y. Liu, Y. Wang, Y. Dai, Z. Dong, Z. Cheng, Z. Zhang and Y. Liu, *J. Alloys Compd.*, 2022, **907**.
63. B. Y. Kim, D. H. Lee, J.-Y. Lee and J.-I. Yun, *Electrochem. Commun.*, 2010, **12**, 1005-1008.
64. C. Liao, B. Cai, X. Wang, S. Chen, G. Chen and J. Lin, *J. Rare Earths*, 2020, **38**, 427-435.
65. S. Yang, J. Wang, H. Wang and X. Lai, *Ionics*, 2016, **22**, 1337-1342.
66. J. Wang, M. Li, W. Han, Z.-Y. Liu, X.-G. Yang, Y. Sun and M.-L. Zhang, *Rare Met.*, 2018, **41**, 1394-1402.
67. P. Cao, M. Zhang, W. Han, Y. Yan, S. Wei and T. Zheng, *J. Rare Earths*, 2011, **29**, 763-767.
68. Y. Castrillejo, P. Fernández, M. R. Bermejo, E. Barrado and A. M. Martínez, *Electrochim. Acta*, 2009, **54**, 6212-6222.
69. L. Massot, H. Meskine, M. Gibilaro and P. Chamelot, *J. Fluorine Chem.*, 2022, **257-258**.
70. T. Jiang, N. Wang, S.-M. Peng, M. Li, W. Han and M.-L. Zhang, *J. Alloys Compd.*, 2016, **658**, 198-209.
71. Y.-s. Yang, M.-l. Zhang, W. Han, P.-y. Sun, B. Liu, H.-l. Jiang, T. Jiang, S.-m. Peng, M. Li, K. Ye and Y.-d. Yan, *Electrochim. Acta*, 2014, **118**, 150-156.
72. H. Tang, Y.-D. Yan, M.-L. Zhang, X. Li, W. Han, Y. Xue, Z.-J. Zhang and H. He, *Electrochim. Acta*, 2013, **107**, 209-215.
73. D.-B. Ji, T.-Q. Yin, Y.-D. Yan, M.-L. Zhang, P. Wang, Y.-H. Liu, J.-N. Zheng, Y. Xue, X.-Y. Jing and W. Han, *RSC Advances*, 2016, **6**, 29353-29364.
74. Y. Yang, M. Zhang, W. Han, H. Jiang, M. Li, K. Ye and Y. Yan, *J. Solid State Electrochem.*, 2013, **18**, 843-850.
75. G. XIE, K. EMA and Y. ITO, *J. Appl. Electrochem.*, 1993, **23**, 753-759.
76. T. Nohira, H. Kambara, K. Amezawa and Y. Ito, *J. Electrochem. Soc.*, 2005, **152**, C183-C189.
77. K. Yasuda, S. Kobayashi, T. Nohira and R. Hagiwara, *Electrochim. Acta*, 2013, **106**, 293-300.
78. H. Hua, K. Yasuda, H. Konishi and T. Nohira, *J. Electrochem. Soc.*, 2021, **168**.
79. L. Wang, Y.-L. Liu, K. Liu, S.-L. Tang, L.-Y. Yuan, L.-L. Su, Z.-F. Chai and W.-Q. Shi, *Electrochim. Acta*, 2014, **147**, 385-391.
80. Y.-L. Liu, L.-Y. Yuan, G.-A. Ye, L. Kui, L. Zhu, M.-L. Zhang, Z.-F. Chai and W.-Q. Shi, *Electrochim.*

Acta, 2014, **147**, 104-113.
81. K. Liu, Y.-L. Liu, L.-Y. Yuan, X.-L. Zhao, Z.-F. Chai and W.-Q. Shi, *Electrochim. Acta*, 2013, **109**, 732-740.
82. L.-X. Luo, Y.-L. Liu, N. Liu, K. Liu, L.-Y. Yuan, Z.-F. Chai and W.-Q. Shi, *RSC Advances*, 2015, **5**, 69134-69142.
83. K. Liu, Y.-L. Liu, L.-Y. Yuan, X.-L. Zhao, H. He, G.-A. Ye, Z.-F. Chai and W.-Q. Shi, *Electrochim. Acta*, 2014, **116**, 434-441.
84. Y. Castrillejo, M. R. Bermejo, A. I. Barrado, R. Pardo, E. Barrado and A. M. Martínez, *Electrochim. Acta*, 2005, **50**, 2047-2057.
85. M. R. Bermejo, F. de la Rosa, E. Barrado and Y. Castrillejo, *J. Electroanal. Chem.*, 2007, **603**, 81-95.
86. Y. Castrillejo, A. Vega, M. Vega, P. Hernández, J. A. Rodriguez and E. Barrado, *Electrochim. Acta*, 2014, **118**, 58-66.
87. Y. Wang, M. Li, W. Han, M. Zhang, Y. Yang, Y. Sun, Y. Zhao and Y. Yan, *J. Solid State Electrochem.*, 2015, **19**, 3629-3638.
88. X. Li, Y.-D. Yan, M.-L. Zhang, H. Tang, D.-B. Ji, W. Han, Y. Xue and Z.-J. Zhang, *Electrochim. Acta*, 2014, **135**, 327-335.
89. Y. Chen, K. Ye and M. Zhang, *J. Rare Earths*, 2010, **28**, 128-133.
90. H. Hong, Q. Yang and G. Liu, *Acta Sci Nat Univ Sunyatseni*, 1990, **29**, 129.
91. K. Yasuda, S. Kobayashi, T. Nohira and R. Hagiwara, *Electrochim. Acta*, 2013, **92**, 349-355.
92. P. Chamelot, L. Massot, C. Hamel, C. Nourry and P. Taxil, *J. Nucl. Mater.*, 2007, **360**, 64-74.
93. T. Iida, T. Nohira and Y. Ito, *Electrochim. Acta*, 2003, **48**, 1531-1536.
94. K. Yasuda, K. Kondo, T. Nohira and R. Hagiwara, *J. Electrochem. Soc.*, 2014, **161**, D3097-D3104.
95. L. M, L. W, H. W, Z. ML and Y. YD, *Chem J Chin Univ*, 2014, **35**, 2662-2667.
96. T. Iida, T. Nohira and Y. Ito, *Electrochim. Acta*, 2001, **46**, 2537-2544.
97. H. Konishi, T. Nohira and Y. Ito, *J. Electrochem. Soc.*, 2001, **148**, C506-C511.
98. S. Kobayashi, T. Nohira, K. Kobayashi, K. Yasuda, R. Hagiwara, T. Oishi and H. Konishi, *J. Electrochem. Soc.*, 2012, **159**, E193-E197.
99. H. Konishi, K. Mizuma, H. Ono, E. Takeuchi, T. Nohira and T. Oishi, *ECS Transactions*, 2012, **50**, 561-569.
100. L. M, S. TT, H. W, W. SS, Z. ML, Y. YD and Z. M, *Chin J Inorg Chem*, 2015, **31**, 177.
101. G. XIE, K. EMA and Y. ITO, *J. Appl. Electrochem.*, 1993, **23**, 753-759.
102. S. Hikino, G. Xie, K. Ema and Y. Ito, *J. Electrochem. Soc.*, 1992, **139**, 1820.
103. S. Vandarkuzhali, N. Gogoi, S. Ghosh, B. Prabhakara Reddy and K. Nagarajan, *Electrochim. Acta*, 2012, **59**, 245-255.
104. D. B. Ji, Y. D. Yan, M. L. Zhang, X. Li, X. Y. Jing, W. Han, Y. Xue, Z. J. Zhang and T. Hartmann, *Electrochim. Acta*, 2015, **165**, 211-220.
105. K. Liu, Y.-L. Liu, L.-Y. Yuan, L. Wang, L. Wang, Z.-J. Li, Z.-F. Chai and W.-Q. Shi, *Electrochim. Acta*, 2015, **174**, 15-25.
106. V. Smolenski and A. Novoselova, *Electrochim. Acta*, 2012, **63**, 179-184.
107. W. Shidong, L. Quan, Y. Xiushen, S. Qingguo and W. Zhijian, *Rare Metal Materials and Engineering*, 2015, **44**, 1623-1628.
108. M.-l. Zhang, P. Cao, W. Han, Y.-d. Yan and L.-j. Chen, *Transactions of Nonferrous Metals Society of China*, 2012, **22**, 16-22.
109. M. Zhang, Y. Yang, W. Han, M. Li, Y. Sun and Y. Yan, *Energy Procedia*, 2013, **39**, 375-381.
110. L. Chen, M. Zhang, W. Han, Y. Yan and P. Cao, *J. Rare Earths*, 2012, **30**, 159-163.
111. X. Ji, C. Wu, S. Jan, Z. Wang and X. Jin, *Electrochem. Commun.*, 2019, **103**, 27-30.
112. Y. Sun, M. Zhang, W. Han, Y. Yan, Y. Yang and Y. Sun, *J. Rare Earths*, 2013, **31**, 192-197.
113. M. Gibilaro, L. Massot, P. Chamelot and P. Taxil, *J. Nucl. Mater.*, 2008, **382**, 39-45.
114. Y. Gao, Y. Shi, X. Liu, C. Huang and B. Li, *Electrochim. Acta*, 2016, **190**, 208-214.
115. M. Gibilaro, L. Massot, P. Chamelot, L. Cassayre and P. Taxil, *Electrochim. Acta*, 2009, **55**, 281-287.
116. B. K. Kim, S. Choi and B. G. Park, *Electrochim. Acta*, 2022, **406**.
117. G. Yu, L. Zhou, F. Liu, S. Pang, D. Chen, H. Zhao and Z. Zuo, *J. Rare Earths*, 2022, **40**, 1945-1952.
118. W. Li, H. Zhang, J. Yu, K. Jiang, A. Novoselova, V. Smolenski, Q. Liu, J. Zhu, M. Zhang and J. Wang, *Intermetallics*, 2023, **162**.
119. M. F. Simpson and P. Sachdev, *Nuclear Engineering and Technology*, 2008, **40**, 175-182.
120. J. Veliscek-Carolan, *J. Hazard. Mater.*, 2016, **318**, 266-281.
121. D.-W. Yang, S.-L. Jiang, Y.-L. Liu, J.-S. Geng, M. Li, L. Wang, Z.-F. Chai and W.-Q. Shi, *Sep. Purif.*

Technol., 2022, **281**, 119853.
122. K. Liu, Y.-L. Liu, Z.-F. Chai and W.-Q. Shi, *J. Electrochem. Soc.*, 2017, **164**, D169-D178.
123. L. Luo, Y. Liu, N. Liu, K. Liu, J. Pang, L. Yuan, Z. Chai and W. Shi, *Science China Chemistry*, 2017, **60**, 813-821.
124. Q. Rayée, T. Doneux and C. Buess-Herman, *Electrochim. Acta*, 2017, **237**, 127-132.
125. J.-M. Hur, S. M. Jeong and H. Lee, *Electrochem. Commun.*, 2010, **12**, 706-709.
126. T. Yin, Y. Liu, D. Yang, Y. Yan, G. Wang, Z. Chai and W. Shi, *J. Electrochem. Soc.*, 2020, **167**, 122507.
127. C. Kwon, J. Kang, S. H. Noh and B. Han, *Journal of Industrial and Engineering Chemistry*, 2019, **70**, 94-98.
128. G. De Córdoba, A. Laplace, O. Conocar and J. Lacquement, *J. Nucl. Mater.*, 2009, **393**, 459-464.
129. S. Im, S.-L. Shang, N. D. Smith, A. M. Krajewski, T. Lichtenstein, H. Sun, B. J. Bocklund, Z.-K. Liu and H. Kim, *Acta Mater.*, 2022, **223**, 117448.
130. Y. Wang, Q. Liu, S. Zhang, Y. Liu, Y. Wang, Y. Dai, Z. Dong, Z. Cheng, X. Cao, Y. Chen, Z. Zhang and Y. Liu, *Sep. Purif. Technol.*, 2022, **294**, 120972.
131. V. Smolenski, A. Novoselova, A. Osipenko, M. Kormilitsyn and Y. Luk'yanova, *Electrochim. Acta*, 2014, **133**, 354-358.
132. V. Smolenski, A. Novoselova, A. Osipenko and A. Maershin, *Electrochim. Acta*, 2014, **145**, 81-85.
133. V. Smolenski, A. Novoselova, V. Volkovich, Y. Luk'yanova, A. Osipenko, A. Bychkov and T. R. Griffiths, *J. Radioanal. Nucl. Chem.*, 2016, **311**, 687-693.
134. W. Li, X. Zhang, J. Wang, L. Chen, Q. Sun, W. Han, M. Li and Y. Wei, *J. Solid State Electrochem.*, 2023, **27**, 927-937.
135. M. Xu, V. Smolenski, Q. Liu, A. Novoselova, K. Jiang, J. Yu, J. Liu, R. Chen, H. Zhang, M. Zhang and J. Wang, *J. Electrochem. Soc.*, 2020, **167**.
136. H. Zhang, Q. Liu, A. Novoselova, V. Smolenski, J. Yu, J. Zhu, Y. Yan, M. Zhang and J. Wang, *J. Electroanal. Chem.*, 2022, **927**.
137. W. Han, W. Wang, Y. Zhang, Y. Wang, M. Li and Y. Sun, *International Journal of Energy Research*, 2021, **45**, 8577-8592.
138. L. Ding, X. Wang, Y. Yan, V. Smolenski, W. Xu, A. Novoselova, Y. Xue, F. Ma and X. Zhang, *J. Rare Earths*, 2023, **41**, 1250-1257.
139. W. Han, W. Wang, M. Li, Y. Meng, W. Ji and Y. Sun, *J. Electrochem. Soc.*, 2020, **167**.